Soft Matter

RSC Publishing

PAPER

View Article Online
View Journal | View Issue

Cite this: *Soft Matter*, 2013, **9**, 9608

Bioinspired assembly of functional block-copolymer nanotemplates†

I.-Hong Lin,[b] Chih-Chia Cheng,*[b] Wei-Tsung Chuang,[c] Jem-Kun Chen,[d] U.-Ser Jeng,[c] Fu-Hsiang Ko,[e] Chih-Wei Chu,[f] Chih-Feng Huang[g] and Feng-Chih Chang*[a]

Received 9th July 2013
Accepted 30th July 2013

DOI: 10.1039/c3sm51870a

www.rsc.org/softmatter

A new concept on bioinspired assembly of functional diblock copolymers, capable of forming different microstructures through nucleobase-induced supramolecular interactions, has been explored. In this paper, a new series of uracil-functionalized poly(ε-caprolactone)-*b*-(4-vinylbenzyl uracil)s (PCL-*b*-PVBU) have been prepared which exhibit a high self-complementary ability in solution and solid states owing to the formation of uracil–uracil pairs by induced hierarchical self-assembly. The ordered morphologies of PCL-*b*-PVBU diblock copolymers changed from a lamellar, hexagonally packed cylinder to a sphere with respect to the content of the hydrogen bond segment. Moreover, we further show that the PCL segment could be easily extracted by enzymatic degradation, leading to a cylinder porous structure of long-range order, which gives a facile method for the fabrication of uracil-functionalized nanotemplates. In addition, bio-complementary PCL-*b*-PVBU/9-hexadecyladenine (AC16) hierarchical supramolecular complexes formed through strong cooperative hydrogen bonding between the uracil group of PVBU and the adenine group of A-C16. When the mixing ratios of PCL-*b*-PVBU/AC16 differ from the stoichiometric ratio, these complexes self-assemble into well-ordered lamellar and hexagonal structures; the changing morphology at different AC16 loadings reveals that the molecular structures of the PCL-*b*-PVBU/AC16 complexes are readily tailored.

Introduction

Molecular organization *via* the formation of complementary hydrogen bonding provides a powerful tool for creating well-defined nanostructures.[1] These materials utilize non-covalent interactions similar to those found in bio-molecules such as protein, DNA, and RNA to direct and modulate their 3-D topology.[2] Multiple-hydrogen-bonding interactions are moderately strong and highly directional within biomimetic polymers which can create unique physical properties, such as high specificity, controlled affinity, and reversibility.[3] However, controlling the supramolecular structure with secondary (and higher) bonding through different hydrogen-bonding motifs still remains a challenging task.[4] Thus, the study of non-covalent interactions and the resulting higher structures at the molecular level is the key to appending the design aspect of bio-inspired materials.

In order to utilize the complementary nature of nucleobase pairs, numerous reports regarding the effect on material properties of the placement of chain ends on polymers or small molecules using supramolecular motifs have been presented.[1d,5] One of the most elegant and successfully employed motifs for supramolecular polymerizations is the quadruple hydrogen-bonded ureidopyrimidone developed by Sijbesma, Meijer, and co-workers which strongly self-dimerizes through four hydrogen bonds arranged in donor–donor–acceptor–acceptor (DDAA) sites.[6] Attaching this motif to the chain ends of a macromonomer results in enhancement of polymer properties in both solution and solid states. It is also possible to place nucleobases on polymer side-chains.[7] For instance, Rotello and co-workers[7a,8] prepared poly(styrene-*co*-chloromethylstyrene) random copolymers where chloromethylstyrenes along the polymer backbone served as functional handles to provide the recognition sites. In addition, these copolymers could also be functionalized non-covalently using hydrogen bonding.

Block copolymers constitute a special class of materials capable of self-assembling into a series of long-range ordered nanostructures owing to their mutual incompatibility.[9] Polymers with comb-shaped architecture also display the propensity to self-organize due to repulsion between the backbone and the

[a]*Department of Materials and Optoelectronic Science, National Sun Yat-Sen University, Kaohsiung 80424, Taiwan. E-mail: changfc1973@gmail.com*

[b]*Institute of Applied Chemistry, National Chiao-Tung University, Hsinchu 30050, Taiwan. E-mail: chihchia.ac95g@nctu.edu.tw*

[c]*National Synchrotron Radiation Research Center, Hsinchu 30076, Taiwan*

[d]*Department of Materials Science and Engineering, National Taiwan University of Science and Technology, Taipei 10607, Taiwan*

[e]*Department of Materials Science and Engineering, National Chiao-Tung University, Hsinchu 30050, Taiwan*

[f]*Research Center for Applied Sciences, Academia Sinica, Taipei 11529, Taiwan*

[g]*Department of Chemical Engineering, National Chung-Hsin University, Taichung 40227, Taiwan*

† Electronic supplementary information (ESI) available. See DOI: 10.1039/c3sm51870a

short side chains.[10] A variety of ordered nanostructures can be constructed if the comb architecture is introduced into the block copolymer by selectively complexing one of the blocks in a coil–coil diblock copolymer with a surfactant.[11] The "supramolecular comb–coil diblock copolymer" systems construct polymeric structures with two length scales of self-organization: one gives rise to the length of scale of several nanometers formed due to the microphase separation between comb and coil blocks, and the other yields a smaller length scale lamellar structure with an interlamellar distance of several nanometers from the segregation between the polymer backbone and the amphiphilic tail in the comb block. The supramolecular comb–coil concept was pioneered and widely investigated by Ikkala and co-workers.[12] In addition to the rich variety of hierarchical nanostructures, the mesomorphic order of the comb block also exerts an interesting influence on the self-organization behavior of the coil block. For instance, the relatively small-scale lamellar mesophase was found to induce the formation of large-scale lamellae domains organized by the coil block in a supramolecular comb–coil diblock through the complexation of polystyrene-*block*-poly(4-vinylpyridine) (PS-*b*-P4VP) with zinc dodecylbenzenesulfonate.[12b]

In our previous study,[13a,b] the biocomplementary interactions between a nucleobase-like side-chain homopolymer and alkylated nucleobases formed through thymine–adenine (T–A) and uracil–adenine (U–A) base pairs have been studied and the complex possessed well-ordered lamellar structures of which *d*-spacing was controlled by the degree of crystallization of the alkyl side chains. Recently,[13c] we reported the synthesis and assembly behavior of heteronucleobase-functionalized poly(ε-caprolactone) (PCL) indicating that the attachment of multiple hydrogen-bonding units to chain ends of PCL resulted in phase separation and a substantial increase in the viscosity. In this study, a new series of poly(ε-caprolactone)-*block*-poly[1-(4-vinylbenzyl uracil)] (PCL-*b*-PVBU) diblock copolymers were synthesized through the combination of ring-opening polymerization (ROP) of ε-caprolactone (ε-CL) followed by nitroxide-mediated radical polymerization (TEMPO) of vinylbenzyl chloride (4-VBC) and then quantitative copper-catalyzed Huisgen 1,3-dipolar cycloaddition reactions[14] between an azide and an alkyne. These newly synthesized diblock copolymers possess unique dynamic behavior and self-assembled structures. Moreover, the segment of the PCLs within block copolymers can be easily extracted by enzymatic degradation with lipase, revealing mesoporous material allowing a high surface area and a dense set of PVBU brushes at the cylinder walls. In addition, an amphiphilic alkylated nucleobase, 9-hexadecyladenine (AC16), was synthesized and incorporated into the RNA-like diblock copolymer to form comb–coil diblock copolymers through biocomplementary uracil–adenine (U–A) base pairs. The specific interactions and diverse phase changes within these PCL-*b*-PVBU/AC16 blends were also investigated.

Experimental section

A series of uracil-functionalized PCL-*b*-PVBUs with different average lengths of the hydrogen bond segments were prepared by "click chemistry" of PCL-*b*-PVBAz in the presence of propargyl uracil using CuBr/PMDETA as a catalyst system. WAXS/SAXS data were collected using the BL17A1 wiggler beamline of the National Synchrotron Radiation Research Center (NSRRC), Taiwan. All samples were sealed between two Kapton windows (thickness: 12 μm) and measured at room temperatures. Samples for TEM investigations were prepared by ultra-thin sections of the polymer film on a carbon-coated copper grid. The general materials, synthetic procedures, NMR data, GPC measurements, DSC experiments, enzymatic degradation and instrumentation used in this work are described in more detail in the ESI.†

Results and discussion

Synthesis of uracil-functionalized block copolymers with different average lengths of the hydrogen bond segments

In the first stage of preparing this new block copolymer, the click reaction was employed by introducing a concentrated solution of azide-functionalized prepolymer to a vigorously stirring solution of PCL-*b*-PVBAz at 60 °C. CuBr and PMDETA were added and the reaction was carried out at 60 °C for 24 h. The uracil-grafted block copolymer of PCL-*b*-PVBU with 1,2,3-trizaole linkages (Scheme 1a) was passed through neutral aluminum oxide and purified by dialysis in DMF, followed by precipitation into methanol, and white semicrystalline powders were obtained (the detailed synthetic strategy is described in the ESI†). Successful incorporation of the uracil was confirmed using ^{1}H NMR and FT-IR spectroscopy. IR spectra of the azide-functionalized PCL-*b*-PVBAz revealed the presence of a pronounced azide stretch at 2100 cm^{-1} and a methylene resonance at δ 4.2 ppm in the ^{1}H NMR spectrum (Fig. S1 and S2†) also appeared. When the triazole was formed from the reaction between N^1-(prop-2-yne-1-yl)uracil and PCL-*b*-PVBAz, the azide stretch at 2100 cm^{-1} completely disappeared. In addition, six new resonances of uracil were also observed in the ^{1}H NMR spectrum of PCL-*b*-PVBU at 11.2 ppm (r, –CO–N*H*–CO–), 8.0 ppm (l, *H*C═C–), 7.8 ppm (p, –N–C*H*–), and 5.5 ppm (q, –CO–C*H*–). Methylene resonances (o,–N–CH_2–) associated with heteroatoms overlapped with the methine protons in the uracil

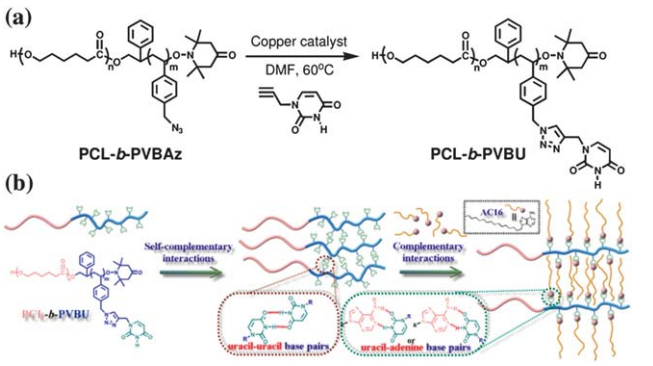

Scheme 1 (a) Synthetic procedures of the uracil-functioned PCL-*b*-PVBU copolymer. (b) Graphical representation of supramolecular assemblies formed by self-complementary and complementary hydrogen-bonding units.

repeat units at 5.5 ppm (q, –CO–C*H*–). Molecular weights and molecular weight distributions of the PCL-*b*-PVBU polymers are listed in Table S1.† The number-average molecular weights are calculated from the ^{1}H NMR integration ratios of the methylene signal on the PCL polymer backbone (–OC═OCH_2–, 3.9–4.2 ppm) to the signal on the methylene protons (–CH_2–N–N–, 5.0–5.2 ppm). To further evaluate the effect of hydrogen-bonding associations on solution aggregation, the solution of PCL-*b*-PVBU in DMF was examined using gel-permeation chromatography, and the results are shown in Fig. S3.† An azide-containing PCL-*b*-PVBAz precursor was prepared from the PCL macroinitiator, which possessed narrow polydispersity and monomodal GPC traces. Interestingly, the observed multimodal of the GPC trace of PCL-*b*-PVBU can be attributed to the formation of the supramolecule in the solution. This observation indicates that these nucleobase units are able to form complexes through the intermolecular uracil–uracil (U–U) interaction in dynamic equilibrium under flow and they result in a high degree of aggregation (Scheme 1b). In addition, the intriguing hydrogen bond feature led us to investigate the self-assembly of PCL-*b*-PVBU in the bulk state.

Self-assembly and enzymatic degradation of uracil-functionalized block copolymers in the bulk state

Hydrogen bond-mediated self-assembly can be used as a bottom-up approach for the development of advanced structures.[5] If these hydrogen bonds are strong enough, supramolecular polymerization can be applied to the objects directly.[5c] We performed differential scanning calorimetry (DSC), wide- and small-angle X-ray scattering (WAXS and SAXS) and transmission electron microscopy (TEM) to understand the self-assembly behavior of PCL-*b*-PVBU. Fig. S4† displays the second-run DSC thermograms of PCL-*b*-PVBU with various PVBU contents. The pure PCL-*b*-PVBU block copolymer exhibited two glassy transitions (T_gs) and a melting temperature (T_m) because of the immiscibility between the PCL and PVBU segments. The T_gs of the PCL and PVBU blocks were *ca.* −60 and 165 °C, while the T_m of the PCL block was *ca.* 55 °C. The T_g of the amorphous PVBU (165 °C) block was substantially higher than the melting point of the PCL crystallites. Therefore, the PVBU amorphous block played the role as hard confinement[15] and this block copolymer system possessed moderate segregation limits [high $(\chi N)_{T_c}$ value] for PCL crystallization under vitrified nanometer-scale confinement. In addition, the T_g of the PVBU block increased while the T_g of the PCL block remained nearly unchanged when the amount of the PVBU block was increased. Therefore, the incorporation of uracil into the phenyl side chain significantly influences the thermal properties of the block copolymer due to strong inter-association hydrogen bonds between the uracil groups.

Further investigation into the self-assembly behaviors of these copolymers was carried out through WAXS measurements (Fig. S5†). The immiscible and crystallized PCL blocks in all copolymers possessed two distinct diffraction peaks at $2\theta = 21.5$ and 23.8°, corresponding to (110) and (200) reflections, respectively. These diffraction peaks revealed orthorhombic packing and perfect crystallographic orientation of the crystalline structure.[16] Furthermore, the WAXS pattern of PCL-*b*-PVBU displayed several amorphous halos centered at $2\theta = 4.53°$ (d = 1.83 nm), 19.0° (d = 0.47 nm), and 29.3° (d = 0.31 nm), corresponding to distances between the main chains and phenyl rings.[13a,b,17] The introduction of U–U interaction expands the interchain spacing and reduces the intramolecular distance between phenyl rings.[17b] The intermolecular distance is increased because the size of the side chains is increased after the incorporation of uracil while the intramolecular distance is reduced as a result of the attraction caused by the U–U interaction. Furthermore, the reflection peak at $2\theta = 26.8°$ (d = 0.34 nm) indicates that stacks of nucleobase are formed through π–π interactions within these "hard" domains of U–U aggregation. This observation suggests that the immiscibility between PCL and nucleobase hard segment units induces their self-assembly and results in micro-phase separation. Thus, the one-dimensional SAXS measurement is employed to analyze the detailed microstructural information.

Fig. 1 shows low-q SAXS profiles of the PCL-*b*-PVBU observed at room temperature. For CU1 and CU2, the SAXS intensity displays a series of lattice peaks with the positions of 1 : 2 : 3, indicating that they possessed a lamellar phase with a characteristic domain spacing (D) of 33.1 nm calculated from the primary peak position (q_m) *via* $D = 2\pi/q_m$. The CU3 also shows a long-range order structure with a ratio of peak positions of 1 : √3 : 2, revealing an ordered phase of hexagonally packed cylinders. In the case of CU4, however, the long period spacing decreased significantly to 29.9 nm and well-defined spherical microstructures were also observed, corresponding to a position ratio of 1 : √2 : √3. In other words, the long-period distance would be reduced because of the increase in the fraction of uracil units attached to the PVBU block, and the intermolecular association would be increased as a result of the phase transition caused by U–U interactions. Moreover, TEM micrographs shown in Fig. 2 provide real-space morphological observation of

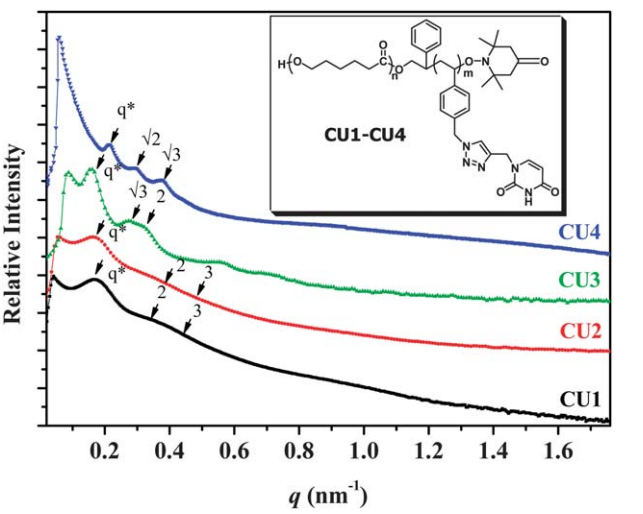

Fig. 1 Representative room-temperature SAXS profiles of the PCL-*b*-PVBU diblock copolymer. Arrows are a guide for the eyes.

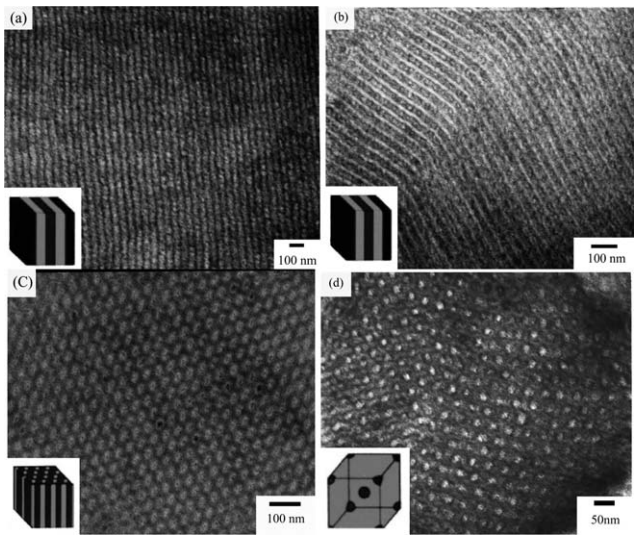

Fig. 2 TEM images of solution-casting films of (a) pure CU1, (b) pure CU3, and (c) pure CU4 stained with RuO_4. (a) and (b) correspond to lamellar structures, (c) represents a hexagonal cylinder structure, and (d) represents a sphere.

the structure which is consistent with those observed from SAXS. After RuO_4 staining, the dark and light domains represent the phenyl and PCL microdomains, respectively. Fig. 2a and b show the lamellar structures within CU1 and CU2 which are regular with a lamellar period of *ca.* 35–45 nm. When the content of the PVBU block is increased, the morphology shifted from lamellae to a hexagonal cylinder structure as shown in Fig. 2c which presents the hexagonal PCL cylinders dispersed within the PVBU matrix in pure CU3. The average microdomain radius and the distance between spheres from TEM micrographs are *ca.* 30–40 nm. In Fig. 2d, spheres (bright domains) with a radius of *ca.* 30 nm and an inter-distance of *ca.* 10 nm are observed where the disorder dark domains correspond to the PVBU phase. Based on the above discussion, the increase in the fraction of the PVBU within the polymer matrix leads to a change in the distance between PVBU phases due to the assembled PVBU through U–U interactions (Scheme 1b). In addition, we can also conclude that there exist different long-range order nanostructures derived by the incompatibility between the covalently connected blocks.

Through appropriate design of compositions of PCL-*b*-PVBU diblock copolymers, the formation of the different morphologies can be controlled, enabling us to tailor the surface activity of the nanostructures for specific requirements and applications. Therefore, the segment of the PCLs within block copolymers can be easily extracted by enzymatic degradation with lipase, giving a facile method for the fabrication of uracil-functionalized nanotemplates. (The degradation process is described in more detail in the ESI.†) The changes of the ^1H NMR spectra of PCL-*b*-PVBU films before and after degradation are shown in Figs. S6 and S7a.† *Pseudomonas* lipase is known as the degradation enzyme for PCL,[18] and it was used as the biocatalyst to degrade the PCL segments in this study. After 7 days in the presence of lipase, the peak at 3.9–4.2 ppm disappeared completely, while the peak at 5.2–5.6 ppm remained unchanged. The relative stability of the chemical composition during degradation can be explained by the fact that only PCL segments are degraded but PVBU segments can escape from the degradation medium. Further evidence for the PCL segment removal was observed based on the WAXD data. Fig. S7b† represents the WAXD patterns before (black-colored) and after (red-colored) enzymatic treatment of PCL-*b*-PVBU. The crystalline peaks in WAXD patterns were weakened during the degradation. Therefore it is concluded that the crystallinity of PCL was decreased during degradation. Finally, TEM was used to analyze the porosity of the block copolymer as a template. Fig. 2c shows the cylinder structure before enzymatic treatment. Because of RuO_4 staining, the PVBU microdomains appear dark, whereas the PCL microdomains appear bright. Subsequently, the PCL block of the PCL-*b*-PVBU bulk samples was degraded by the enzyme. Fig. S8† shows the treatment of the sample without RuO_4 staining. The relative thicknesses of the layers have not essentially changed during the degradation, indicating that the structure remains and does not collapse. Thus, we further suggested that this uracil-functionalized nanotemplate is now possible to create fully addressable nanostructures from the selective binding of complementary DNA strands, to probe and modify the structure of the guest DNA.

Biocomplementary interaction induced morphology transition in uracil-functionalized PCL-*b*-PVBU/AC16 complexes

Molecular recognition is an interesting phenomenon that can result in various morphological changes.[19] To evaluate the ability of PCL-*b*-PVBU to form complexes with AC16 through complementary U–A hydrogen bonding (Scheme 1b), the self-assembly through molecular recognition in the bulk state was examined using FT-IR spectroscopy. Fig. S9a† illustrates the N–H stretching region of the FT-IR spectra of the CU1/AC16 complexes. The characteristic peaks are the free amide NH group (3500 cm^{-1}) of PVBU and those involved in U–U (3173 cm^{-1}) interactions. The presence of the band at 3500 cm^{-1} indicates that a fraction of the uracil side groups of the PCL-*b*-PVBU diblock copolymer was not involved in U–U interactions. The intensity of the free amide N–H stretching vibration at 3500 cm^{-1} decreased as the amount of AC16 increased, indicating that the PVBU segment associated with its complement, AC16, and A–U interactions were more favorable than either U–U or A–A interactions. FTIR spectra revealed the presence of bands at 3350 and 3295 cm^{-1} corresponding to hydrogen-bonded amide N–Hs of CU1/AC16,[20] indicating that the uracil groups of PVBU are highly complementary to the adenine group of AC16. In addition, upon heating from room temperature to 180 °C, the signals at 3350 and 3295 cm^{-1} corresponding to hydrogen bonded N–H stretching were shifted to higher wavenumber, and the free amide N–H stretching at 3501 cm^{-1} appeared gradually for the 80/20 complex (Fig. S9b†), suggesting a change in the nature of the hydrogen bonding at that temperature.

The thermal properties of the CU1/AC16 complexes were examined by DSC (Fig. S10†). The glass transition temperature

(T_g) of the PVBU segment was ~163 °C and the melting point (T_m) of AC16 was 120 °C. The T_g of the 80/20 complex was 151 °C, implying that the complementary hydrogen bonding indeed occurred in the CU1/AC16 complex. The T_g was reduced by the presence of the side-chain alkyl groups of AC16 to constitute a disorder phase, and a less nonstoichiometric amount of AC16 side alkyl chains led to a uniform glass transition.[13a,21] As a weight fraction of AC16 greater than 0.3, the T_g was not detected, probably due to the high side-chain crystallinity of the AC16. The melting temperatures of the CU1/AC16 complexes showed an increasing trend upon increasing the AC16 content in the complex as shown in Fig. S10.† The increase of the melting temperature indicates that the side alkyl chains formed a more regular crystalline phase and were arranged perpendicular to the amorphous phase sheets as the AC16 content was increased. At a 30/70 CU1/AC16 weight ratio, the T_m shifted significantly to 118 °C because of the presence of excess AC16. The intriguing behavior led us to investigate the microstructures of these complexes in more detail through SAXS and TEM measurements.

SAXS profiles of CU1/AC16 blends were obtained at room temperature to confirm the formation of microphase-separated morphologies, and the results are shown in Fig. 3a. The pure CU1 block copolymer shows the first-order scattering broad peak corresponding to a Bragg spacing of 34.2 nm (the average spacing between the PCL and the neighboring PVBU microphase). CU1/AC16 = 80/20 also shows a long-range order structure with a ratio of peak positions of 1 : 2 : 3, revealing an order phase of a lamellar structure. The CU1/AC16 = 70/30 blend gives 1 : $\sqrt{7}$ ratio positions, indicating a hexagonally packed cylinder. The blend with higher AC16 content (CU1/AC16 = 50/50 wt%) possesses broad peaks, indicating the absence of a long-range order structure. The lower degree of order of the large-scale structure in CU1/AC16 resulted from perturbation by the higher extent of crystallization of AC16 in the system. It is known that the crystallization may perturb the long-range order of the melt mesophase of block copolymers.[22] However, SAXS results indicate that the 80/20 and 70/30 complexes could form well-ordered lamellar and hexagonal structures, respectively, although we obtained a relatively disordered structure at higher AC16 contents, *i.e.*, for AC16 contents greater than 50%. To further determine the interlamellar distance in the lamellar array accurately, the primary diffraction peak was detected in the WAXS experiments. Fig. 3b shows the X-ray scattering intensity curves in the q range of 0.25–2 Å^{-1}. CU1 does not have a peak in the low q region, while the complex has peaks at q^*, $2q^*$, and $3q^*$, indicating a lamellar structure with a long period of *ca.* 25 Å. Based on previous data obtained from FTIR, TEM and SAXS, the presence of peaks in the low q region indicates that this complex possesses an internal smaller domain within these PVBU/AC16 layers (Scheme 1b).

Fig. 4a shows the TEM micrograph of CU1/AC16 = 80/20, displaying a lamellar structure with a long period of *ca.* 30–40 nm. Also in this case, there is no common alignment of the lamellae, and a considerable number of defects remain in the sample. Interestingly, the morphological transformation can be

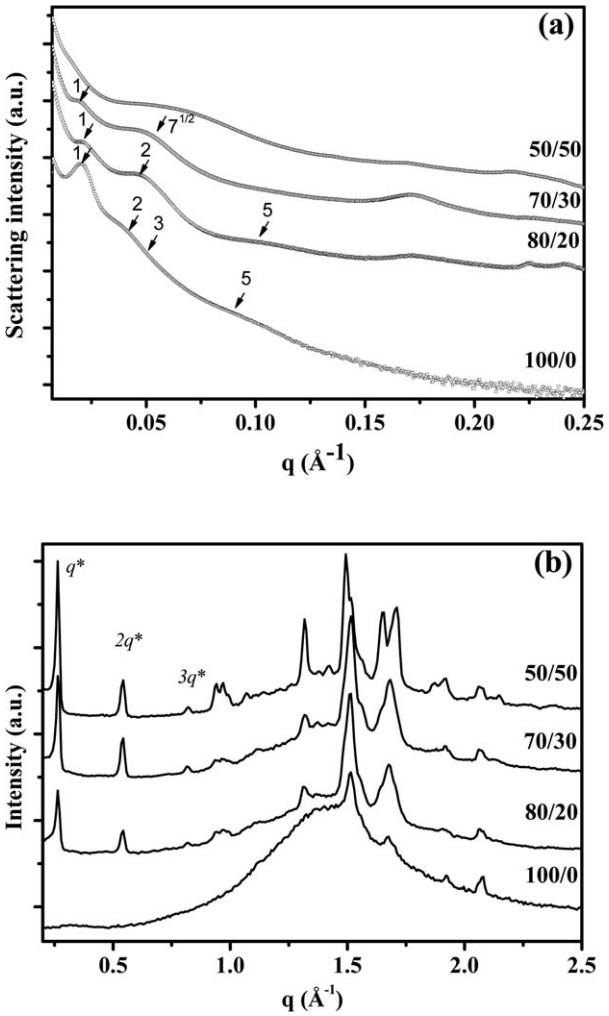

Fig. 3 (a) X-ray intensity patterns of PCL-*b*-PVBU/AC16 complexes with different weight fractions in the (a) q < 0.25 Å^{-1} and (b) q = 0.25–2.5 Å^{-1} regions. The magnitude of the scattering vector is given by $q = (4\pi/\lambda)\sin\theta$, where 2θ is the scattering angle and λ = 1.54 Å. Arrows are a guide for the eyes.

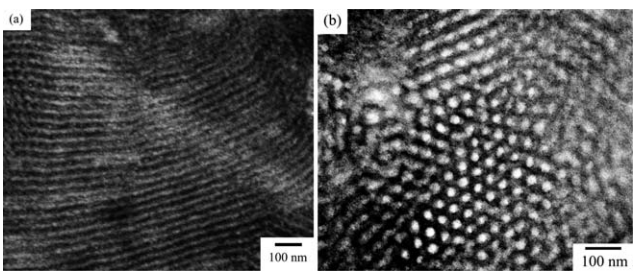

Fig. 4 (a) Transmission electron micrographs of solution-cast films of CU1/AC16 = 80/20 wt%, and (b) CU1/AC16 = 70/30 wt% blend stained with RuO_4. (a) corresponds to a lamellar structure. (b) represents a hexagonal cylinder structure.

observed from the lamellar structure to the hexagonal cylinder structure when CU1 is blended with 30% AC16 as shown in Fig. 4b. The lamellar structure can be formed if PVBU and the AC16 complexes form interlamellar layers whereas the hexadecyl alkyl chains are extended.[23] According to the above, we can depict a hierarchical self-organization, *i.e.* lamellar-within-lamellar and

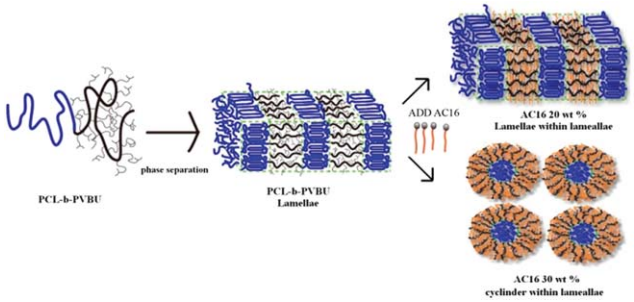

Scheme 2 Morphology change in PCL-*b*-PVBU/AC16 blends with the increase of AC16 content.

cylinder-with-lamellar structure (Scheme 2). However, the smaller structure within the PVBU/AC16 domain was unable to be resolved with TEM. It should be noted that the crystalline uncomplexed AC16 has several peaks in the wide angle q range whereas the pure block copolymer shows only a 2θ of 21.5 and 23.8° for the (110) and (200) reflections.

Conclusions

In summary, ring-opening polymerization, controlled living free radical (nitroxide-mediated) polymerizations, and click chemistry were employed to synthesize biomimetic diblock copolymer PCL-*b*-PVBU. Complementarity between the guest molecules and polymer functionalities plays a critical role in directing the segregation preference of the molecules to the different structure transitions. We found that the removal of the PCL segment was successful, and the microstructures did not collapse due to the glass PVBU phase, revealing mesoporous material allowing a high surface area and a dense set of uracil brushes at the cylinder walls. In a complementary study, we demonstrated a simple supramolecular way of constructing self-organizing comb-crystalline diblock copolymers with two length scales by combining diblock copolymers with hydrogen-bonding complementary molecules. The micrograph analyses indicate that different compositions of PCL-*b*-PVBU/AC16 blends result in different microphase-separated structures through the mediation of hydrogen-bonding interactions. The concept allows a rich variety of morphologies and phase transitions from recognition unit-functionalized block copolymer scaffolds by modifying the block lengths and the amount of supramolecular complexes. Therefore, these complexes could be applied widely as a means of manipulating the morphologies and biochemical surface properties of biomaterials, because hydrogen bonding might provide them with biocompatibility. Thus, we expect that such materials could be further developed to provide medical and biotechnological applications.

Acknowledgements

We thank National Synchrotron Radiation Research Center (NSRRC, Taiwan) for the support in the SAXS and WAXS measurements. This study was supported financially by the National Science Council, Taiwan (contract no. NSC-101-2221-E-009-030-).

Notes and references

1 (*a*) M. J. Krische and J.-M. Lehn, *Struct. Bonding*, 2000, **96**, 3; (*b*) L. J. Prins, D. N. Reinhoudt and P. Timmerman, *Angew. Chem., Int. Ed.*, 2001, **40**, 2382; (*c*) R. P. Sijbesma and E. W. Meijer, *Chem. Commun.*, 2003, 5; (*d*) S. Sivakova and S. J. Rowan, *Chem. Soc. Rev.*, 2005, **34**, 9; (*e*) J. L. Sessler and J. Jayawickramarajah, *Chem. Commun.*, 2005, 1939.

2 (*a*) E. A. Fogleman, W. C. Yount, J. Xu and S. L. Craig, *Angew. Chem., Int. Ed.*, 2002, **41**, 4026; (*b*) K. Yamauchi, A. Kanomata, T. Inoue and T. E. Long, *Macromolecules*, 2004, **37**, 3519; (*c*) D. R. Vutukuri, S. Basu and S. Thayumanavan, *J. Am. Chem. Soc.*, 2004, **126**, 15636.

3 (*a*) A. K. Boal, F. Ilhan, J. E. DeRouchey, T. Thurn-Albrecht, T. P. Russell and V. M. Rotello, *Nature*, 2000, **404**, 746; (*b*) J. Bernard, F. Lortie and B. Fenet, *Macromol. Rapid Commun.*, 2009, **30**, 83; (*c*) K. E. Feldman, M. J. Kade, E. W. Meijer, C. J. Hawker and E. J. Kramer, *Macromolecules*, 2009, **42**, 9072; (*d*) S. K. Yang, A. V. Ambade and M. Weck, *Chem. Soc. Rev.*, 2011, **40**, 129.

4 (*a*) M. Muthukumar, C. K. Ober and E. L. Thomas, *Science*, 1997, **277**, 1225; (*b*) S. Zou, H. Schroenherr and G. J. Vancso, *Angew. Chem., Int. Ed.*, 2005, **44**, 956; (*c*) J. T. Roland and Z. Guan, *J. Am. Chem. Soc.*, 2004, **126**, 14328.

5 (*a*) K. Yamauchi, J. R. Lizotte and T. E. Long, *Macromolecules*, 2002, **35**, 8745; (*b*) S. Rieth, C. Baddeley and J. D. Badjic, *Soft Matter*, 2007, **3**, 137; (*c*) G. ten Brinke, J. Ruokolainen and O. Ikkala, *Adv. Polym. Sci.*, 2007, **207**, 113.

6 (*a*) R. P. Sijbesma, F. H. Beijer, L. Brunsveld, B. J. B. Folmer, J. H. K. K. Hirschberg, R. F. M. Lange, J. K. L. Lowe and E. W. Meijer, *Science*, 1997, **278**, 1601; (*b*) F. H. Beijer, R. P. Sijbesma, H. Kooijman, A. J. Spek and E. W. Meijer, *J. Am. Chem. Soc.*, 1998, **120**, 6761; (*c*) B. J. B. Folmer, R. P. Sijbesma, H. Kooijman, A. L. Spek and E. W. Meijer, *J. Am. Chem. Soc.*, 1999, **121**, 9001.

7 (*a*) R. Shenhar, H. Xu, B. L. Frankamp, T. E. Mates, A. Sanyal, O. Uzun and V. M. Rotello, *J. Am. Chem. Soc.*, 2005, **127**, 16318; (*b*) W. H. Binder, C. Kluger, C. J. Straif and G. Friedbacher, *Macromolecules*, 2005, **38**, 9405; (*c*) B. D. Mather, M. B. Baker, F. L. Beyer, M. A. G. Berg, M. D. Green and T. E. Long, *Macromolecules*, 2007, **40**, 6834; (*d*) R. McHale and R. K. O'Reilly, *Macromolecules*, 2012, **45**, 7665.

8 (*a*) T. H. Galow, F. Ilhan, G. Cooke and V. M. Rotello, *J. Am. Chem. Soc.*, 2000, **122**, 3595; (*b*) A. K. Boal, T. H. Galow, F. Ilhan and V. M. Rotello, *Adv. Funct. Mater.*, 2001, **11**, 461; (*c*) K. Das, H. Nakade, J. Penelle and V. M. Rotello, *Macromolecules*, 2004, **37**, 310; (*d*) C. Subramani, S. Dickert, Y.-C. Yeh, M. T. Tuominen and V. M. Rotello, *Langmuir*, 2011, **27**, 1543.

9 I. W. Hamley, *The Physics of Block Copolymers*, Oxford University Press, New York, 1998.

10 N. A. Platé and V. P. Shibaev, *Comb-Shaped Polymers and Liquid Crystals*, Plenum Press, New York, 1987.

11 (*a*) O. Ikkala and G. ten Brinke, *Science*, 2002, **295**, 2407; (*b*) H. L. Chen, J. S. Lu, C. H. Yu, C. L. Yeh, U. S. Jeng and W. C. Chen, *Macromolecules*, 2007, **40**, 3271; (*c*) W. S. Chiang, C. H. Lin, B. Nandan, C. L. Yeh, M. H. Rahman, W. C. Chen and H. L. Chen, *Macromolecules*, 2008, **41**, 8138.

12 (*a*) J. Ruokolainen, R. Mäkinen, M. Torkkeli, T. Mäkelä, R. Serimaa, G. ten Brinke and O. Ikkala, *Science*, 1998, **280**, 557; (*b*) S. Valkama, T. Ruotsalainen, H. Kosonen, J. Ruokolainen, M. Torkkeli, R. Serimaa, G. ten Brinke and O. Ikkala, *Macromolecules*, 2003, **36**, 3986; (*c*) S. Valkama, H. Kosonen, J. Ruokolainen, T. Haatainen, M. Torkkeli, R. Serimaa, G. ten Brinke and O. Ikkala, *Nat. Mater.*, 2004, **3**, 872; (*d*) W. van Zoelen, T. Asumaa, J. Ruokolainen, O. Ikkala and G. ten Brinke, *Macromolecules*, 2008, **41**, 3199; (*e*) J. Korhonen, T. Verho, P. Rannou and O. Ikkala, *Macromolecules*, 2010, **43**, 1507.

13 (*a*) C. C. Cheng, C. F. Huang, Y. C. Yen and F. C. Chang, *J. Polym. Sci., Part A: Polym. Chem.*, 2008, **46**, 6416; (*b*) C. C. Cheng, Y. C. Yen, Y. S. Ye and F. C. Chang, *J. Polym. Sci., Part A: Polym. Chem.*, 2009, **47**, 6388; (*c*) I. H. Lin, C. C. Cheng, Y. C. Yen and F. C. Chang, *Macromolecules*, 2010, **43**, 1245.

14 (*a*) R. Huisgen, in *1,3-Dipolar Cycloaddition Chemistry*, ed. A. Padwa, Wiley, New York, 1984, vol. 1, p. 1; (*b*) R. Huisgen, *Pure Appl. Chem.*, 1989, **61**, 613.

15 (*a*) L. Zhu, S. Z. D. Cheng, B. H. Calhoun, Q. Ge, R. P. Quirk, E. L. Thomas, B. S. Hsiao, F. Yeh and B. Lotz, *J. Am. Chem. Soc.*, 2000, **122**, 5957; (*b*) P. Huang, L. Zhu, Y. Gau, Q. Ge, A. J. Jing, W. Y. Chen, R. P. Quirk, S. Z. D. Cheng, E. L. Thomas, B. Lotz, B. S. Hsiao, C. A. Avilaorta and I. Sics, *Macromolecules*, 2004, **37**, 3689; (*c*) Y. S. Sun, T. M. Chung, Y. J. Li, R. M. Ho, B. T. Ko, U. S. Jeng and B. Lotz, *Macromolecules*, 2006, **39**, 5782.

16 C. L. He, J. R. Sun, M. X. Deng, X. S. Chen and X. B. Jing, *Biomacromolecules*, 2004, **5**, 2042.

17 (*a*) A. J. Waddon and E. B. Coughlin, *Chem. Mater.*, 2003, **15**, 4555; (*b*) J. Wu, T. S. Haddad, G. M. Kim and P. T. Mather, *Macromolecules*, 2007, **40**, 544.

18 T. Nie, Y. Zhao, Z. Xie and C. Wu, *Macromolecules*, 2003, **36**, 8825.

19 W. H. Binder and R. Zirbs, *Adv. Polym. Sci.*, 2007, **207**, 1.

20 Y. Kyogoku, R. C. Lord and A. Rich, *J. Am. Chem. Soc.*, 1967, **89**, 496.

21 (*a*) M. Ballauff, *Makromol. Chem., Rapid Commun.*, 1986, 7407; (*b*) E. A. Ponomarenko, D. A. Tirrell and W. J. MacKnight, *Macromolecules*, 1998, **31**, 1584; (*c*) S. Zhou, Y. Zhao, Y. Cai, Y. Zhou, D. Wang, C. C. Han and D. Xu, *Polymer*, 2004, **45**, 6261.

22 (*a*) Y. L. Loo, R. A. Register and A. J. Ryan, *Phys. Rev. Lett.*, 2000, **84**, 4120; (*b*) H. L. Chen, J. C. Wu, T. L. Lin and J. S. Lin, *Macromolecules*, 2001, **34**, 6936.

23 J. Ruokolainen, J. Tanner, G. ten Brinke, O. Ikkala, M. Torkkeli and R. Serimaa, *Macromolecules*, 1995, **28**, 7779.

